APPLICATION OF PARAMETRIC PSD METHODS FOR ROTOR CAGE FAULT DETECTION OF INDUCTION MOTORS

Lahcène NOUREDDINE **Omar TOUHAMI**

Department of Electrical Engineering, Amar Thlidji University, Laghouat, Algeria
n.lahcene@mail.lagh-univ.dz
Research Laboratory of Electrotechnics, High National Polytechnic College, Algiers, Algeria
Omar.touhami@enp.edu.dz

***Abstract**: This paper presents some experimental results obtained for the diagnosis of rotor broken bars in three squirrel cage induction motors by the analysis of current signatures using parametric PSD methods, these signatures are detected on line by using a sensing board designed on our electrotechnical laboratory of research.*

***Key words:** MCSA, PSD, parametric methods, broken rotor bars, fault diagnsois.*

1. Introduction

Three-phase squirrel cage induction motors are the work horses of industry and are the most widely used electrical machines. In an industrialized nation, they can typically consume between 40 to 50% of all the generated capacity of that country [1]. A condition monitoring system which can predict and identify the fault condition is the need of the age to prevent such unwanted breakdown time. The MCSA (Motor Current Signature Analysis) technique is found one of the most frequently used technique to identify the fault condition [2]. This paper focuses on experimental results to prove that MCSA Technique can identify the good and cracked rotor bar in three phase squirrel cage induction motors under load conditions.

Spectral estimation techniques are widely adopted in machine diagnosis. Typically, three main subclasses can be defined: nonparametric methods, parametric methods, and high-resolution methods [3].

- Nonparametric methods include conventional Fourier analysis, optimal band pass filtering analysis, Periodogram, and Welch. These methods do not solve the limits of the frequency resolution of the classical Fourier analysis.
- Parametric methods are based on the estimation of a linear time invariant system from noise by autoregressive-moving-average (ARMA) model, such as Yule–Walker, Burg, Covariance, and modified Covariance. These methods have improved performances although they are affected by the signal-to-noise ratio (SNR) level.
- High-resolution methods include techniques such as multiple signal classification (MUSIC) and Eigenvector. These methods can detect frequencies with low SNR and compute the autocorrelation matrix, and its Eigen-values can be separated into signal and noise spaces. These methods define a Pseudo-spectrum function with large peaks that are subspace frequency estimates, and they are commonly used in the communication area. They have been recently introduced into the area of induction machine diagnosis by the application of the MUSIC method.

2. Parametric methods

Parametric methods can yield higher resolutions than nonparametric methods in cases when the signal length is short. These methods use a different approach to spectral estimation; instead of trying to estimate the PSD directly from the data, they model the data as the output of a linear system driven by white noise, and then attempt to estimate the parameters of that linear system.

The most commonly used linear system model is the all-pole model, a filter with all of its zeroes at the origin in the z-plane. The output of such a filter for white noise input is an autoregressive (AR) process.

For this reason, these methods are sometimes referred to as AR methods of spectral estimation.

The AR methods tend to adequately describe spectra of data that is "peaky," that is, data whose PSD is large at certain frequencies. The data in many practical applications (such as speech) tends to have "peaky spectra" so that AR models are often useful. In addition, the AR models lead to a system of linear equations which is relatively simple to solve.

2.1. Yule–walker method

It is assumed that the data {$x(0)$,$x(1)$, . . . ,$x(N-1)$} are observed. In the Yule–Walker method, or the autocorrelation method as it is sometimes referred to, the AR parameters are estimated by minimizing an estimate of prediction error power.

$$\text{Variance} = \rho = \frac{1}{N}\sum_{n=-\infty}^{\infty}\left|x(n)+\sum_{k=1}^{p}a(k)x(n-k)\right|^2 \quad (1)$$

The samples of the $x(n)$ process which are not observed (i.e., those not in the range $0 \le n \le N-1$) are set equal to zero in Eq. (5). The estimated prediction error power is minimized by differentiating Eq. (5) with respect to the real and imaginary parts of the $a(k)$'s. This may be done by using the complex gradient to yield [4,5].

$$\frac{1}{N}\sum_{n=-\infty}^{\infty}\left(x(n)+\sum_{k=1}^{p}a(k)x(n-k)\right)x^*(n-l)=0 \quad (2)$$

With: $l = 1,2,...., p$

This set of equations in terms of autocorrelation function estimates becomes:

$$r_p + R_p a = 0 \quad (3)$$

Where:

$$r(k)=\begin{cases}\frac{1}{N}\sum_{n=0}^{N-1-k}x^*(n)x(n+k), & k=0,1,...,p\\ r^*(-k), & k=(-p+1),(-p+2),...,-1\end{cases} \quad (4)$$

From Eq. (7) the AR parameter estimates are found as:

$$a = -R_p^{-1}r_p \quad (5)$$

The estimate of the white noise variance σ2 is calculated as:

$$\sigma^2 = r(0)+\sum_{k=1}^{p}a(k)r(-k) \quad (6)$$

From the estimates of the autoregressive parameters, power spectral density estimation is given as:

$$P(f) = \frac{\sigma^2}{\left|1+\sum_{k=1}^{p}a_k(k)e^{-j2\pi fk}\right|^2} \quad (7)$$

2.2. Burg method

The Burg Method belongs to the class of parametric methods and it is based on an autoregressive (AR) model for the PSD estimation. The underlying system is described by the following difference equation:

$$x[n] = -\sum_{k=1}^{p}a_k x[n-k]+e[n] \quad (8)$$

where *x[n]* is the observed output of the system, *e[n]* is the unobserved input data and the a_k are its coefficients. The input *e[n]* is considered as a zero mean white noise process with unknown variance σ^2, and p is the order of the system. This model is commonly referred as AR(p).

The a_k are determined minimizing the forward and backward prediction errors in the least square sense. The PDS estimation is obtained from the following equation:

$$P_B(f) = \frac{E_p}{\left|1+\sum_{k=1}^{p}a_p e^{-j2\pi fk}\right|^2} \quad (9)$$

where E_p is the total least-square error of order *p*. The major advantages of the Burg Method are its high frequency resolution, the AR model is always stable, and is computationally very efficient. It exhibits, however, several limitations: for high signal to noise ratios line splitting may appear in the PDS and frequency shifting from the true frequency occurs especially for short data record [4,5].

2.3. Covariance method

The only difference between the covariance method and the Yule–Walker method is the range of summation in the prediction error power estimate. In the covariance method all the data points needed to compute the prediction error power estimate. No zeroing of the data is necessary. The AR parameter estimates as the solution of the equations can be written [4,5]:

$$\begin{bmatrix}c(1,0)\\ \vdots\\ c(p,0)\end{bmatrix}+\begin{bmatrix}c(1,1) & \cdots & c(1,p)\\ \vdots & \ddots & \vdots\\ c(p,1) & \cdots & c(p,p)\end{bmatrix}\begin{bmatrix}a(1)\\ \vdots\\ a(p)\end{bmatrix}=\begin{bmatrix}0\\ \vdots\\ 0\end{bmatrix} \quad (10)$$

Where:

$$c(j,k)=\frac{1}{N-p}\sum_{n=p}^{N-1}x^*(n-j)x(n-k) \qquad (11)$$

From Eq. (11) the AR parameter estimates are found as:

$$a=-C_p^{-1}c_p \qquad (12)$$

The white noise variance is estimated as:

$$\sigma^2=c[0,0]+\sum_{k=1}^{p}a[k]c[0,k] \qquad (13)$$

From the estimates of the AR parameters, PSD estimation is formed as:

$$P_{\text{cov}}(f)=\frac{\sigma^2}{\left|1+\sum_{k=1}^{p}a_k(k)e^{-j2\pi fk}\right|^2} \qquad (14)$$

2.4. Modified Covariance method

To derive the estimator, suppose that we are given the data *x(n)*, *n*=0,1,., *N*-1, and let us consider the forward and backward linear prediction estimates of order *m* , as

$$\hat{x}(n)=-\sum_{k=1}^{m}a_m(k)x(n-k) \qquad (15)$$

$$\hat{x}(n-m)=-\sum_{k=1}^{m}a_m^*(k)x(n+k-m) \qquad (16)$$

and the corresponding forward and backward errors $f_m(n)$ and $g_m(n)$ as $f_m(n)=x(n)-\hat{x}(n)$ and $g_m(n)=x(n-m)-\hat{x}(n-m)$, The least square error is

$$\varepsilon_m=\sum_{n=m}^{N-1}\left[|f_m(n)|^2+|g_m(n)|^2\right] \qquad (17)$$

To find the prediction coefficients that minimize ε_m, the derivative of ε_m with respect to $a_m^*(l)$. equal to zero for *l = 1,2,...,m*. Hence

$$\frac{\partial\varepsilon_m}{\partial a_m^*(l)}=\sum_{n=m}^{N-1}\left[f_m(n)\frac{\partial[f_m(n)]^*}{\partial a_m^*(l)}+[g_m(n)]^*\frac{\partial g_m(n)}{\partial a_m^*(l)}\right]$$
$$=\sum_{n=m}^{N-1}\left[f_m(n)x^*(n-l)+[g_m(n)]^*x(n-m+l)\right]=0 \qquad (18)$$

Substituting equation (15) to (17) into equation (18) and simplifying we find that the normal equation for the MC method are given by

$$\sum_{k=1}^{m}[c_x(l,k)+c_x(m-k,m-l)]a_m(k)=-[c_x(l,0)+c_x(m,m-l)] \qquad (19)$$

where $c_x(l,k)=\sum_{n=m}^{N-1}x(n-k)x^*(n-l)$ and known as autocorrelation coefficients, which dependent only on the absolute value of the difference between *l* and *k*, i.e. $c_x(l,k)=c_x(|l-k|)$. However the autocorrelation matrix is not Toeplitz but it is symmetric [6].

3. Rotor broken bars related frequencies

The frequencies related to broken bar defects are well known from the literature. They are given by the following expression [7,8]:

$$f_{bb}=(1\pm 2s)f_s \qquad (20)$$

s - rotor slip
f_s - fundamental frequency (Hz)
f_{bb} - broken bar related frequency (Hz)

The lower frequency sideband is linked to the broken bar fault, while the upper sideband frequency is linked to the speed oscillation caused by the rotor defect. In [9] and [10] was demonstrated that broken bar frequencies are actually contained in the sideband frequencies given by:

$$f_{bb}=(1\pm 2ks)f_s \qquad (21)$$

With *k=1,2,3....*

In the present paper attention is given to the first two current components given by eq. (18) with *k=1*. In general, the magnitudes of the remaining frequencies decays very fast and are more difficult to detect. Expressions (17) and (18) show also that the fault related frequencies are very sensitive to the rotor slip. For light load condition (small values for the slip) they are very close to fundamental frequency. Even with high resolution methods their discrimination from the fundamental poses additional difficulties.

4. Experimental results

4.1. Sensors board design

We have designed our sensors board by using three current sensors LA-55P for detect the stator currents of motor and three voltage sensors LV-25M as shown the following figure:

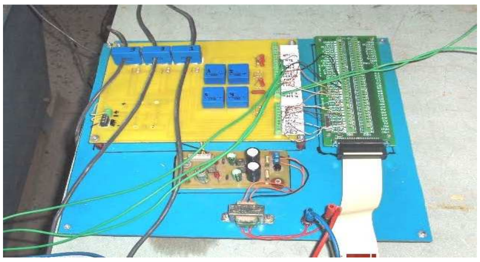

Fig. 1. Sensors board

Each measured signal is simultaneously sampled through channels of a 16 bit, 200 kHz PCI data acquisition (DAQ) board and stored directly into a desktop computer. We have processed and analyzed this data by using Matlab software with sampling frequency 10 KHz.

4.2. Test Bench

In order to evaluate the methods described in section 2 for the case of rotor cage broken bars, several measurements of the stator current of a prototype machine were performed. The prototype machine used has the following rated values: 4kW, 50-Hz, 4-poles, delta connection three-phase squirrel cage industrial induction motors, the first is health, the second with one broken bar, and the third with two broken bars. All the spectra shown have been obtained using built-in functions from the MATLAB DSP Toolbox.

a/

b/ c/

Fig. 2. a/ Experimental bench of induction motors
b/ Rotor with one broken bar
c/ Rotor with two broken bars

The results showed that none of the methods described so far was able to detect rotor defects under load conditions. In all these cases the motors are coupled to a DC generator which acts as a load, and in other side this generator is coupled to the tachymeter for detect rotor speeds as shown figure 2.

4.3. Time-domain results

Fig. 3 show the results of stator currents obtained in healthy, one broken bar, and two broken bars induction motors under load conditions.

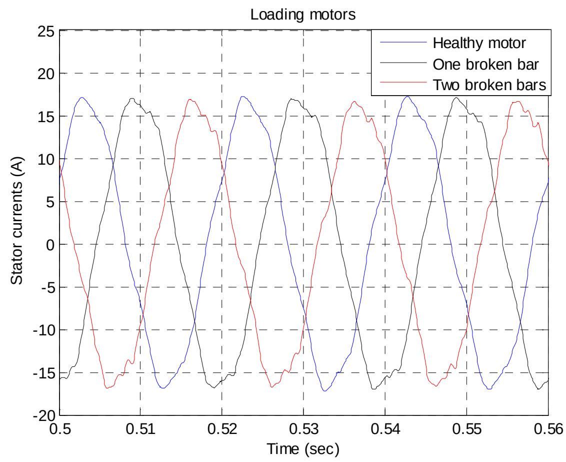

a/

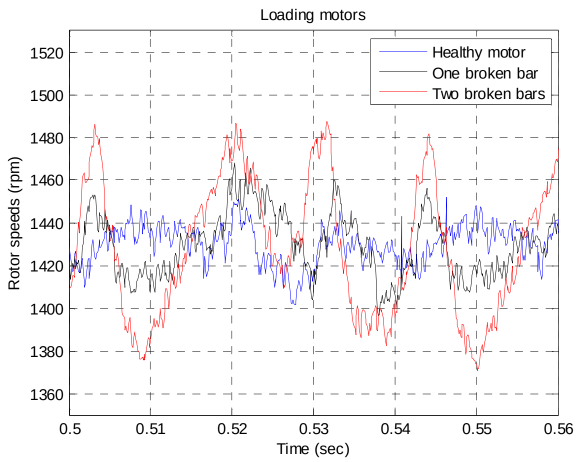

b/

Fig. 3. Time domain results: a/ motors stator currents, b/ motors speeds.

Fig. 3 presents the results of rotor speeds obtained in three cases of motor, in addition the comparison between these speeds.

From the last Fig. 3 b/, it can be seen that speed of rotor with two broken bars is far oscillated than other rotor speeds, this experimental result shows that the oscillation speed is proportional with the number of broken bars.

4.4. PSD estimation results

The parametric methods as Yule walker, Burg, covariance, and Modified Covariance were applied to stator current signatures illustrate in Fig. 3 a/ in the same conditions of full load for our three motors. The spectral diagrams that are obtained by using proposed four methods are given in following figures.

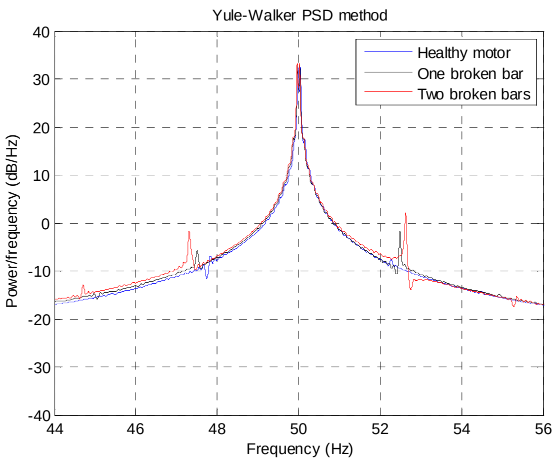

Fig. 4. Yule-Walker PSD results

The Yule-Walker AR method (autocorrelation method) applies window to current signal data and minimizes the forward prediction error in the least squares sense, also it performs as well as other methods for large data records and always produces a stable model. Its disadvantages, it performs relatively poorly for short data records and there are frequency bias for estimates of sinusoids in noise. Because this biased estimate, the autocorrelation matrix is guaranteed to positive-definite, hence nonsingular. For this method, the order of an autoregressive (AR) prediction model used for the signal is 90,000 with data length used (90,001 samples).

The Burg method does not use data windowing, minimizes the forward and backward prediction errors in the least squares sense, with the AR coefficients constrained to satisfy the L-D recursion, high resolution for short data records, and always produces a stable model, being the segment length and the model order its main parameters. Its disadvantages, peak locations highly dependent on initial phase, may suffer spectral line-splitting for sinusoids in noise, or when order is very large, and frequency bias for estimates of sinusoids in noise.

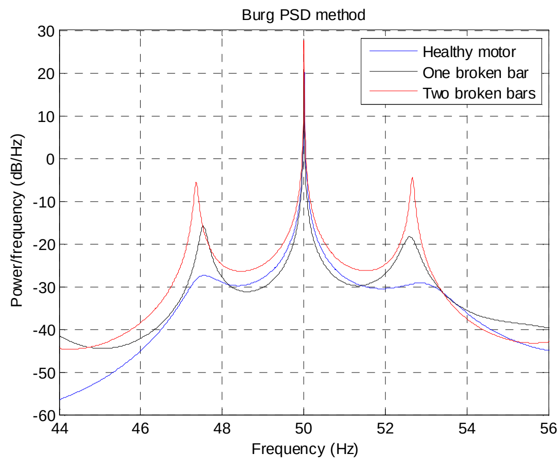

Fig. 5. Burg PSD results

A number of different combinations for these two parameters have been tried and a model order of 2,800 proved to be appropriate for the data length used (5,701 samples).

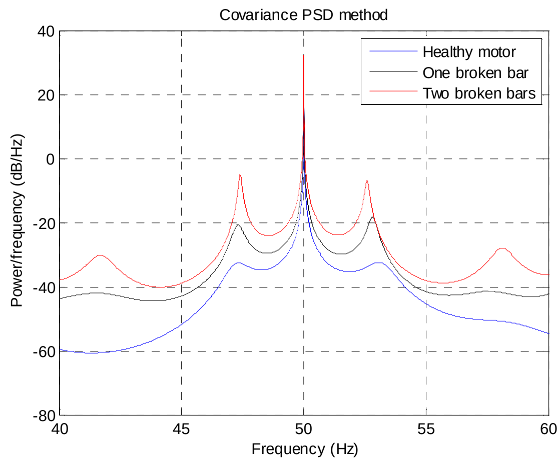

Fig. 6. Covariance PSD results

The Covariance Method does not apply window to data, minimizes the forward prediction error in the least squares sense, better resolution than Y-W for short data records (more accurate estimates), able to extract frequencies from data consisting of *p* or more pure sinusoids. Its disadvantages, may produce unstable models and frequency bias for estimates of sinusoids in noise. Model order must be less than or equal to half the input frame size. The main parameters are the model order 2,200 proved to be appropriate for the data length used (6,001 samples).

The Modified Covariance Method does not apply window to data, minimizes the forward and backward prediction errors in the least squares sense, high resolution for short data records, able to extract frequencies from data consisting of *p* or more pure sinusoids, does not suffer spectral line-splitting.

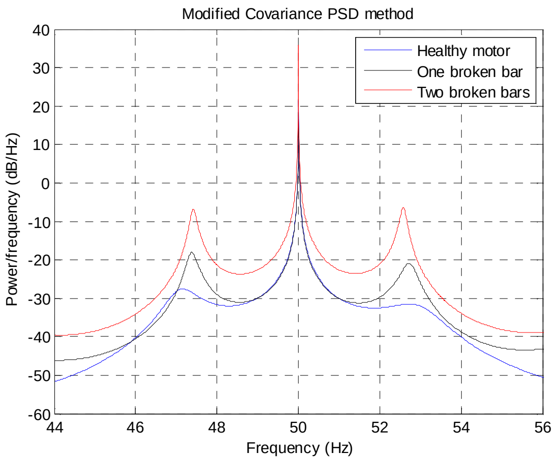

Fig. 7. Modified Covariance PSD results

Its disadvantages, may produce unstable models, peak locations slightly dependent on initial phase, minor frequency bias for estimates of sinusoids in noise. Model order must be less than or equal to 2/3 the input frame size. The main parameters are the model order 2,200 proved to be appropriate for the data length used (6,001 samples).

For all these methods it is possible to determine the model order according to criteria for minimizing the noise influence. However, none of these criteria have been applied to the present case, being the model order determined based on a practical trial and error approach. It was observed that the rotor fault frequencies can be only detected for high model orders. For the cases considered, no fault frequencies appear in the range 44-56 Hz if considered model order under 2,000. The most important issue for the practical use of this method is the correct choice of the model order, which is also influenced by the machine load condition and noise. For use in automated fault detection systems this fact imposes severe difficulties for the adjustment of the parameters set. For load conditions the fault components can be clearly recognized with model order above 2000. The results shown refer to a model order of 2,300. In addition, for load conditions the two main fault components, left (47.4 Hz) and right (52.6 Hz) from the fundamental, have strong peaks and the detection of fault condition is very easy with the correct model order. For both conditions the amplitude of the fault related frequencies increase with increasing load. Finally, from the practical measurements it can be concluded that the performance of the parametric PSD methods are better to confirm the expression of frequencies related to rotor broken bar defects $f_{bb} = (1 \pm 2ks) f_s$ mentioned in section 3 as shown in figures 4 to 7. It can be finally observed that for the case of two broken bars, the fault components of second order, obtained with *k=2* in eq. (21), appear in the yule walker and clearly in the covariance PDS methods at the frequencies 44.7 and 55.3 Hz.

5. Conclusion

For the power quality assessment, it is important to know what the disturbances are in current waveforms. In this paper, four spectral estimation methods which can simultaneously detect all types of harmonics have been presented. It is possible to say that proposed methods will be more effective and successful in filtration applications of all harmonics. It is available to analyze and detect the all type harmonics (integer, inter and sub) at same cases together. We have demonstrated that parametric PSD methods could be instrumental in challenging harmonic detection problems in this study. Our results indicate that the use of covariance and yule walker methods provide relatively better performance in detecting harmonics. Next best performer is the Burg and modified covariance method.

References

1. William T. Thomson, and Mark fenger.: *Current Signature Analysis to Detect IM Faults* IEEE Industry Applications Magazine, pp. 26-34, July/August 2001.
2. R.Saravana Kumara Dr K.K. Raya K.Vinoth Kumar.: *Fault Diagnosis of Industrial Drives Using MCSA Techniques* International Conference On Control, Automation, Communication And Energy Conservation, 4th-6th June 2009.
3. Alberto Bellini, Fiorenzo Filippetti, Carla Tassoni, and Gérard-André Capolino.: *Advances in Diagnostic Techniques for Induction Machines* IEEE Transactions on Industrial Electronics, Vol. 55, No. 12, December 2008.
4. Ahmet Alkan · M. Kemal Kiymik.: *Comparison of AR and Welch Methods in Epileptic Seizure Detection* Journal of Medical Systems, 2006, Volume 30, Number 6, Pages 413-419.
5. Luis A. Pereira, Denis Fernandes, Daniel S. Gazzana, F. B. Libano, and Sergio Haffner.: *Application of the Welch, Burg and MUSIC Methods to the Detection of Rotor Cage Faults of Induction Motors* Transmission & Distribution Conference and Exposition: Latin America, 2006. TDC '06. IEEE/PES.
6. Nursyarizal Mohd Nor, Prof. Dr Ramiah Jegatheesan.: *Application of Modified Covariance Algorithm in State Estimation* Electrical and Electronics Engineering Department, University Technology PETRONAS, Tronoh, Perak, Malaysia.
7. M. Y. Chow.: *Methodologies of Using Neural Network and Fuzzy Logic Technologies for Motor Incipient Fault Detection* World Scientific Publishing, Singapore, 1997.
8. Fenger, M.; Lloyd, B.A.; Thomson, W.T.: *Development of a tool to detect faults in induction motors via current*

signature analysis Cement Industry Technical Conference, May, 2003, pp. 37-46.

9. Filippetti, F.; Franceschini, G.; Tassoni, C.; Vas, P.: *Broken bar detection in induction machines: comparison between current spectrum approach and parameter estimation approach* Industry Applications Society, October, 1994, vol. 1, pp. 95-102.
10. F. Cupertino, E. de Vanna; L. Salvatore, S. Stasi.: *Comparison of Spectral Estimation Techniques Applied to Induction Motor Broken Bars Detection* Symposium on Diagnostics for Electric Machines, Power Electronics and Drives, August 2003, pp. 129-134.